FINITE DIFFERENCE MODELS FOR THE STATIONARY HARMONICS OF ATMOSPHERIC MOTION

M. SANKAR-RAO

The Travelers Research Center, Inc., Hartford, Conn.

ABSTRACT

A finite difference procedure is utilized for the solution of a coupled system of two ordinary differential equations governing the time averaged quasi-geostrophic perturbations in the atmosphere. The seasonal changes in the latitudinal mean state are found to introduce important phase changes and reversals in the asymmetric meridional circulation. A hypothetical latitudinal mean stability profile, which resembles many of the latitudinal mean stability profiles generally used in analytical studies, is found to give acceptable results in many cases. Barotropic models for the zonal mean state are found to be incapable of giving acceptable quantitative results

1. INTRODUCTION

The long-standing debate on the relative importance of the thermal and orographic influences in maintaining the stationary zonally-asymmetric perturbations of the atmosphere cannot yet be considered resolved despite much theoretical effort on this subject. As is well known, the solutions of the linearized approximate potential vorticity equation for the stationary zonally-asymmetric state, which is the basis of most of the theoretical discussions, are controlled not only by the assumed distribution of the forcing due to the thermal, orographic, and transient eddy effects, but also by the assumed form of the basic zonal mean state, rotation, and friction. Even when the forcing functions are assumed to be explicitly known, this equation in its general form is not separable except under certain restrictive assumptions regarding the zonal mean state, the Coriolis parameter f and its variation with latitude β. The theoretical studies up to the recent past naturally fall into four broad groups, depending on the combination of, and assumptions about, the influencing factors considered in each case.

A. Research in which the effect of forcing due only to heating is investigated.

In these works, some or all of the variables of the basic zonal mean state are generally considered either constant or pressure dependent only. f and β are taken as constants. Friction is generally considered. Sometimes when an equivalent barotropic or two-level baroclinic model is used, implicit assumptions are made regarding the variation of even the zonally asymmetric perturbations with pressure. Examples of studies in this group are Smagorinsky [26], Gilchrist [10], Delisle and Harper [6] and Döös [7].[1]

B. Studies in which the effect of forcing due to orography only is investigated.

In these researches, the treatment of the basic zonal mean state, f, β, and friction is similar to that in the thermal case, and here also, implicit assumptions are usually made regarding the variation of the zonally-asymmetric perturbations with pressure. Examples are Queney [18], Charney and Eliassen [4], Bolin [3], Gambo [8, 9], Magata [15], and Kawata [12].

C. Investigations in which attempts are made to study the results of forcing due to a combination of heating, orography, and transient eddy effects, of different spatial scales.

In these studies, also, the treatment of the basic zonal mean state, f, β, and friction is similar to that in the above cases. No assumptions are made regarding the variation of the zonally-asymmetric perturbations with pressure (e.g., Saltzman [20], [21]).

D. Researches in which attention is focused not only on the forcing functions, but also on the latitudinal variation of f and U_0, the zonal mean east-west component of the wind.

Friction is not considered in these works. In some cases, mainly as a mathematical expedient, barotropy, or in effect equivalent barotropy, is forced on the zonal mean state or on both the zonal mean state and the perturbations. Examples of studies of this kind are Kuo [14],[2] Staff Members, Academia Sinica [27], and Barrett [1].

In addition to these theoretical works, a great number of published diagnostic observational results are pertinent to this problem. Examples are Sutcliffe [28], Haurwitz and Craig [11], Saltzman and Peixoto [23], Van Mieghem, Defrise, and Van Isacker [29], Clapp [5], Saltzman and Fleisher [22], and Saltzman and Rao [24].

[1] Döös parameterised one part of the heating by a heating function similar to that used by Mintz [16]. Future advances seem to lie in parameterisations of this kind.

[2] Though Kuo treated a homogeneous problem, his work is of great importance for the question of forced perturbations

Even when the components of the basic zonal mean state are taken as functions of pressure alone, the analytical solution of the resulting coupled system of ordinary differential equations is very laborious and time consuming. Introduction of realistic zonal mean vertical profiles is extremely difficult, if not impossible, in the usual analytical methods. It is the main purpose of this paper to demonstrate a powerful finite difference method which not only reduces the labor to an insignificant amount of computer time, but also opens new possibilities for many kinds of numerical experimentation. As examples, some interesting results will also be discussed.

2. APPROXIMATE EQUATION GOVERNING THE TIME AVERAGED AXIALLY ASYMMETRIC PERTURBATIONS OF THE ATMOSPHERE

We adopt the notation of Saltzman [21] except for the following changes: x^*, y^*, X, Y, Q, H, and the subscript δ of Saltzman, are replaced here by x, y, A_X, A_Y, H, Q and the subscript b, respectively. Also, we further define

$$D_* = \overline{D} - D_0$$
$$K = \Gamma^{-1}$$
$$X = Lx$$
$$Y = Ly$$
$$\xi = p/p_s$$

where

D = any dependent variable
L = any scaling length $\neq 0$
p_s = any scaling pressure $\neq 0$.

With the use of the above notation, the approximate nondimensionalised equations governing the time-averaged axially asymmetric perturbations of the atmosphere, along with the top and bottom boundary conditions, in the X, Y, and ξ system, assume the form (Saltzman [21]).

$$\frac{\partial^2 v_*}{\partial X^2}+\frac{\partial^2 v_*}{\partial Y^2}+\gamma\frac{\partial^2 v_*}{\partial \xi^2}+\delta\frac{\partial v_*}{\partial \xi}+\epsilon v_* = (L^2 F_*)/U_0 \tag{1}$$

$$\frac{\partial v_*}{\partial \xi}+b v_* = dH_* \quad \text{at } \xi=\xi_T \tag{1a}$$

$$\frac{\partial v_*}{\partial \xi}+B v_*+\tau\left(\frac{\partial v_*}{\partial X}-\frac{\partial u_*}{\partial Y}\right)=E\frac{\partial h_*}{\partial X}+NH_* \quad \text{at } \xi=\xi_b \tag{1b}$$

where

$$\gamma=\gamma_{(Y,\xi)}=(-L^2 f^2 p K_0)/p_s^2 R$$

$$\delta=\delta_{(Y,\xi)}=\left(-L^2 f^2 \frac{\partial}{\partial \xi}[pK_0]\right)/p_s R$$

$$\epsilon=\epsilon_{(Y,\xi)}=\frac{L}{U_0}\left[\frac{\partial \eta_0}{\partial Y}+\frac{f}{p_s}\frac{\partial}{\partial \xi}\left(K_0\cdot\frac{\partial T_0}{\partial Y}\right)\right]$$

$$\eta_0=\left[f-\frac{1}{L}\frac{\partial U_0}{\partial Y}\right]$$

$$\left.\begin{aligned} b&=b_{(Y)}=-\frac{p_s R}{U_0 p f}\frac{1}{L}\frac{\partial T_0}{\partial Y}\\ d&=d_{(Y)}=(-p_s R)/U_0 p f\end{aligned}\right\}\text{at } \xi=\xi_T$$

$$\left.\begin{aligned} B&=B_{(Y)}=-\frac{p_s R}{U_0 p f}\frac{1}{L}\frac{\partial T_0}{\partial y}\\ \tau&=\tau_{(Y)}=\frac{g\rho_b C}{K_0 L}\cdot\frac{p_s R}{U_0 p f}\\ E&=E_{(Y)}=-\frac{g\rho_b}{K_0 L}\frac{p_s R}{pf}\\ N&=N_{(Y)}=(-p_s R)/U_0 p f\end{aligned}\right\}\text{at } \xi=\xi_b.$$

In the X and Y directions, we assume periodicity. Also here F_*, H_*, and h_*, which denote the axially asymmetric manifestation of internal and external forcing functions, and γ, δ, ϵ, b, d, B, τ, E, and N, which denote the axially symmetric state, are considered given.

3. MATHEMATICAL PROBLEM

Given the coefficients and forcing functions in (1), (1a), and (1b), the problem is to solve (1) with periodicity conditions in the X and Y directions, while at ξ_T and ξ_b, (1a) and (1b) have to be satisfied respectively. Before considering the relaxation technique which naturally suggests itself for such a problem, we should note that the lower boundary condition (1b) contains a second dependent variable u_* which can be written in terms of v_* through the geostrophic assumption. Then (1), (1a), and (1b) will be in one dependent variable v_* only, but (1b) will be an integro-differential equation. The order change by the introduction of the geopotential will not solve the difficulties completely, because ϵ in the zero order term in (1) is usually *positive* for most of the earth's atmosphere. It is found that under these circumstances the relaxation method cannot be applied to solve (1) with its above-mentioned boundary conditions (Sankar-Rao [25]). Thus mostly for mathematical expediency, we assume that

(Assumption 1) $U_0=U_0(\xi)$, $K_0=K_0(\xi)$, $\frac{\partial T_0}{\partial Y}=\frac{\partial T_0}{\partial Y}(\xi)$

and

(Assumption 2) $\frac{1}{L}\frac{\partial f}{\partial Y}=\beta=\text{constant}$

so that $\gamma=\gamma(\xi)$, $\delta=\delta(\xi)$, $\epsilon=\epsilon(\xi)$ while b, d, B, τ, E, N become constants. Now let us introduce b_K, d_K, B_K, τ_K, E_K, and N_K to denote the new constants b, d, B, τ, E, and N respectively. Also let Ξ, Θ, and Λ represent $\gamma(\xi)$, $\delta(\xi)$, and $\epsilon(\xi)$ respectively. With this notation, (1), (1a), and (1b) take the form

$$\frac{\partial^2 v_*}{\partial X^2}+\frac{\partial^2 v_*}{\partial Y^2}+\Xi\,\frac{\partial^2 v_*}{\partial \xi^2}+\Theta\,\frac{\partial v_*}{\partial \xi}+\Lambda v_*=G_* \tag{2}$$

$$\frac{\partial v_*}{\partial \xi}+b_K v_*=d_K H_* \qquad \text{at } \xi=\xi_T \tag{2a}$$

$$\frac{\partial v_*}{\partial \xi}+B_K v_*+\tau_K\left(\frac{\partial v_*}{\partial X}-\frac{\partial u_*}{\partial Y}\right)=E_K\,\frac{\partial h_*}{\partial Y}+N_K H_* \qquad \text{at } \xi=\xi_b \tag{2b}$$

where

$$G_*=(L^2F_*)/U_0.$$

The simplified problem is now to solve (2) with its prescribed boundary conditions. To this effect, we can now use the double Fourier expansion method which is equivalent to the method of separation of variables.

4. FOURIER EXPANSION AND THE RESULTING SYSTEM OF ORDINARY DIFFERENTIAL EQUATIONS

Assuming that all the time averaged axially asymmetric dependent variables satisfy the Dirichlet conditions, we can expand any such dependent variable D_* as

$$D_*(X, Y, \xi)=\sum_{m=1}^{\infty}\sum_{n=0}^{\infty}\left[D^{\xi}_{1,m,n}\cos\frac{2\pi mX}{l}+D^{\xi}_{2,m,n}\sin\frac{2\pi mX}{l}\right]\cos\frac{2\pi nY}{k}+\left[D^{\xi}_{3,m,n}\cos\frac{2\pi mX}{l}+D^{\xi}_{4,m,n}\sin\frac{2\pi mX}{l}\right]\sin\frac{2\pi nY}{k}.$$

Here l and k are the lengths of the fundamental region in X and Y directions respectively. m and n are wave numbers. The subscripts m and n and superscript ξ indicate that the Fourier coefficients are functions of m, n, and ξ.

Now dropping subscripts m and n, and superscript ξ for convenience in writing and substituting expansions of the above type in (2), (2a), and (2b) we get two coupled systems of ordinary differential equations with ξ as the independent variable (after writing u_* in terms of v_* in (2b) through the geostrophic approximation) as follows, for a single harmonic:

First System

$$\Xi\,\frac{d^2v_1}{d\xi^2}+\Theta\,\frac{dv_1}{d\xi}+(\Lambda-\nu^2)v_1=G_1 \tag{3}$$

$$\frac{dv_1}{d\xi}+b_K v_1=d_K H_1 \qquad \text{at } \xi=\xi_T \tag{3a}$$

$$\frac{dv_1}{d\xi}+B_K v_1+\tau_K\cdot\frac{l\nu^2}{2m\pi}\,v_2=E_K\cdot\frac{2m\pi}{l}\,h_2+N_K H_1 \qquad \text{at } \xi=\xi_b \tag{3b}$$

$$\Xi\,\frac{d^2v_2}{d\xi^2}+\Theta\,\frac{dv_2}{d\xi}+(\Lambda-\nu^2)v_2=G_2 \tag{4}$$

$$\frac{dv_2}{d\xi}+b_K v_2=d_K H_2 \qquad \text{at } \xi=\xi_T \tag{4a}$$

$$\frac{dv_2}{d\xi}+B_K v_2-\tau_K\cdot\frac{l\nu^2}{2m\pi}\,v_1=-E_K\cdot\frac{2m\pi}{l}\,h_1+N_K H_2 \qquad \text{at } \xi=\xi_b. \tag{4b}$$

Here

$$\nu^2=4\pi^2\left[\frac{m^2}{l^2}+\frac{n^2}{k^2}\right].$$

Symbols with subscripts 1 and 2 refer to the Fourier coefficients, which are functions of m, n, and ξ, for the respective dependent variables. We note that the coupling in the first system comes through the friction term.

Second System

The second system is exactly similar to the first; the subscripts 3 and 4 replacing 1 and 2 respectively in the first system.

5. SOME REMARKS

We shall concern ourselves with the first system only because the second system is exactly similar. The first system is generally solved (Smagorinsky [26], Saltzman [20]) by making further analytical assumptions regarding the coefficients, Ξ, Θ, and Λ so that the resulting second order ordinary differential equations contain coefficients which are linear functions of the independent variable and therefore can always be transformed to standard confluent hypergeometric type of equations (cf., Bateman [2], p. 249). At this point, we shall depart from the analytical approach and follow a finite difference method.

We note that the equations (3) and (4) have a singular point at the level where $U_0=0$. Here v_* can be many valued. But in the real atmosphere, such singularities do not exist and v_* remains a single-valued function. At such places where $U_0=0$ in the real atmosphere, other physical processes (neglected here), like virtual viscosity and heat conduction due to molecular and small-scale eddy effects, become dominant. However, at a small but finite distance from this point, the original equations can be expected to hold. So, in the neighborhood of the point where $U_0=0$, we have to use new equations, taking these additional processes into consideration. The nature of these new equations will be different and the point where $U_0=0$ becomes a regular point. In this way, the difficulty with the singularity has been circumvented in previous analytical studies (Kuo [13, 14]: DeLisle and Harper [6]). In the numerical procedure to be described here we do not perform calculations in the neighborhood of this singular point. Thus, in effect, we assume continuity of all the variables across this singular point. In this way, we force regularity on this point. By using a fine enough mesh, we can expect to confine the error introduced by this procedure to a small neighborhood of this point. In this context, the author feels it important to study in the future, by this method, some of the related analytical works, e.g., DeLisle and Harper [6]. Thus, for this finite difference scheme, we shall assume that

(Assumption 3) No point of the finite difference lattice for the region considered coincides with a singular point.

6. FINITE DIFFERENCE METHOD OF SOLUTION

The fundamental difficulty in applying the finite difference technique to solve the system (1) is the coupling, which cannot be broken up by simple addition or subtraction. The first method, naturally suggesting itself, is to take an arbitrary v_2 and solve for v_1 from (3), (3a), and (3b) and take that v_1 and solve for a new v_2 from (4), (4a), and (4b) and to repeat this process until we arrive at stationary values of v_1 and v_2. There is no guarantee that such a process will lead to convergence unless we are able to prove it by numerical analysis. A superior method which takes advantage of the fact that the *upper* boundary conditions are not coupled, will be described now. In this context we shall introduce multiple letter symbols which are like FORTRAN floating point variables.

A. THE FINITE DIFFERENCE INTERIOR EQUATION

The centered difference equation corresponding to (3) can be written at any grid point j as (fig. 1)

$$\mathrm{A2N}(j)v_1(j+1)+\mathrm{B1N}(j)\cdot v_1(j-1)+\mathrm{C0N}(j)\cdot v_1(j)=\mathrm{DFN}(j) \tag{5}$$

where

$$\mathrm{A2N}(j)=2\cdot\Xi(j)-\Theta(j)\cdot\delta\xi$$

$$\mathrm{B1N}(j)=2\cdot\delta\xi^2\cdot\Lambda(j)-4\cdot\Xi(j)-2\cdot\delta\xi^2\nu^2$$

$$\mathrm{C0N}(j)=2\cdot\Xi(j)+\Theta(j)\cdot\delta\xi$$

$$\mathrm{DFN}(j)=2\cdot\delta\xi^2\cdot G_1(j)$$

$\delta\xi$=grid spacing

j=an index referring to grid points from 1 to J.

$$(J-1)\delta\xi=[\xi_T-\xi_b]$$

and $D(j)$=value of any dependent variable D at j. Here, without any loss of generality, we assumed that ξ is decreasing from 1 to J.

The centered difference equation for (4) is written similarly as

$$\mathrm{A2N}(j)v_2(j+1)+\mathrm{B1N}(j)\cdot v_2(j-1)+\mathrm{C0N}(j)\cdot v_2(j)=\mathrm{EFN}(j) \tag{6}$$

Now we consider a one parameter family of solutions for v_1 and v_2 which are of the iterative type (Richtmyer [19], p. 103),

$$v_1(j)=\mathrm{E1N}(j)\cdot v_1(j+1)+\mathrm{F1N}(j)$$

$$v_2(j)=\mathrm{E2N}(j)\cdot v_2(j+1)+\mathrm{F2N}(j)$$

where

$$\mathrm{E1N}(j)=\frac{-\mathrm{A2N}(j)}{[\mathrm{B1N}(j)+\mathrm{C0N}(j)\cdot\mathrm{E1N}(j-1)]} \tag{5.1}$$

$$\mathrm{F1N}(j)=\frac{[\mathrm{DFN}(j)-\mathrm{C0N}(j)\cdot\mathrm{F1N}(j-1)]}{[\mathrm{B1N}(j)+\mathrm{C0N}(j)\cdot\mathrm{E1N}(j-1)]} \tag{5.2}$$

$$\mathrm{E2N}(j)=\frac{-\mathrm{A2N}(j)}{[\mathrm{B1N}(j)+\mathrm{C0N}(j)\cdot\mathrm{E2N}(j-1)]} \tag{6.1}$$

$$\mathrm{F2N}(j)=\frac{[\mathrm{EFN}(j)-\mathrm{C0N}(j)\cdot\mathrm{F2N}(j-1)]}{[\mathrm{B1N}(j)+\mathrm{C0N}(j)\cdot\mathrm{E2N}(j-1)]} \tag{6.2}$$

In order to get E1N(1), F1N(1), E2N(1), and F2N(1) which are necessary to calculate E1N(j), F1N(j), E2N(j), and F2N(j) from (5.1), (5.2), (6.1), and (6.2), we introduce the boundary condition at ξ_T.

B. APPLICATION OF THE UPPER BOUNDARY CONDITION

To introduce the boundary conditions in finite difference form, we will assume that,

(Assumption 4) The dependent variables v_1 and v_2 are continuous across the boundaries at ξ_T and ξ_b so that the interior equation as well as the boundary conditions are to be fulfilled at $j=1$ and at $j=J$.

With this assumption, we can now introduce fictitious points at $j=0$ and $j=J+1$ (see fig. 1). If we write the upper boundary condition at $j=1$ in the centered difference form and require that the iterative type of equations (5) and (6) must hold for any member of the family, we get

$$v_1(1)=\mathrm{E1N}(1)\cdot v_1(2)+\mathrm{F1N}(1) \tag{5a}$$

$$v_2(1)=\mathrm{E2N}(1)\cdot v_2(2)+\mathrm{F2N}(1) \tag{6a}$$

where

$$\mathrm{E1N}(1)=-\frac{[\mathrm{A2N}(1)+\mathrm{C0N}(1)]}{[\mathrm{B1N}(1)-\mathrm{C0N}(1)\cdot\mathrm{G1N}]} \tag{5a.1}$$

$$\mathrm{F1N}(1)=\frac{[\mathrm{DFN}(1)-\mathrm{C0N}(1)\cdot\mathrm{H1N}]}{[\mathrm{B1N}(1)-\mathrm{C0N}(1)\cdot\mathrm{G1N}]} \tag{5a.2}$$

$$\mathrm{E2N}(1)=-\frac{[\mathrm{A2N}(1)+\mathrm{C0N}(1)]}{[\mathrm{B1N}(1)-\mathrm{C0N}(1)\cdot\mathrm{G2N}]} \tag{6a.1}$$

$$\mathrm{F2N}(1)=\frac{[\mathrm{EFN}(1)-\mathrm{C0N}(1)\cdot\mathrm{H2N}]}{[\mathrm{B1N}(1)-\mathrm{C0N}(1)\cdot\mathrm{G2N}]} \tag{6a.2}$$

$$\left.\begin{array}{l}\mathrm{G1N}=2\cdot\delta\xi\cdot b_K\\ \mathrm{G2N}=2\cdot\delta\xi\cdot b_K\\ \mathrm{H1N}=2\cdot\delta\xi\cdot d_K\cdot\mathrm{H}_1\\ \mathrm{H2N}=2\cdot\delta\xi\cdot d_K\cdot\mathrm{H}_2\end{array}\right\}\text{ at } j=1$$

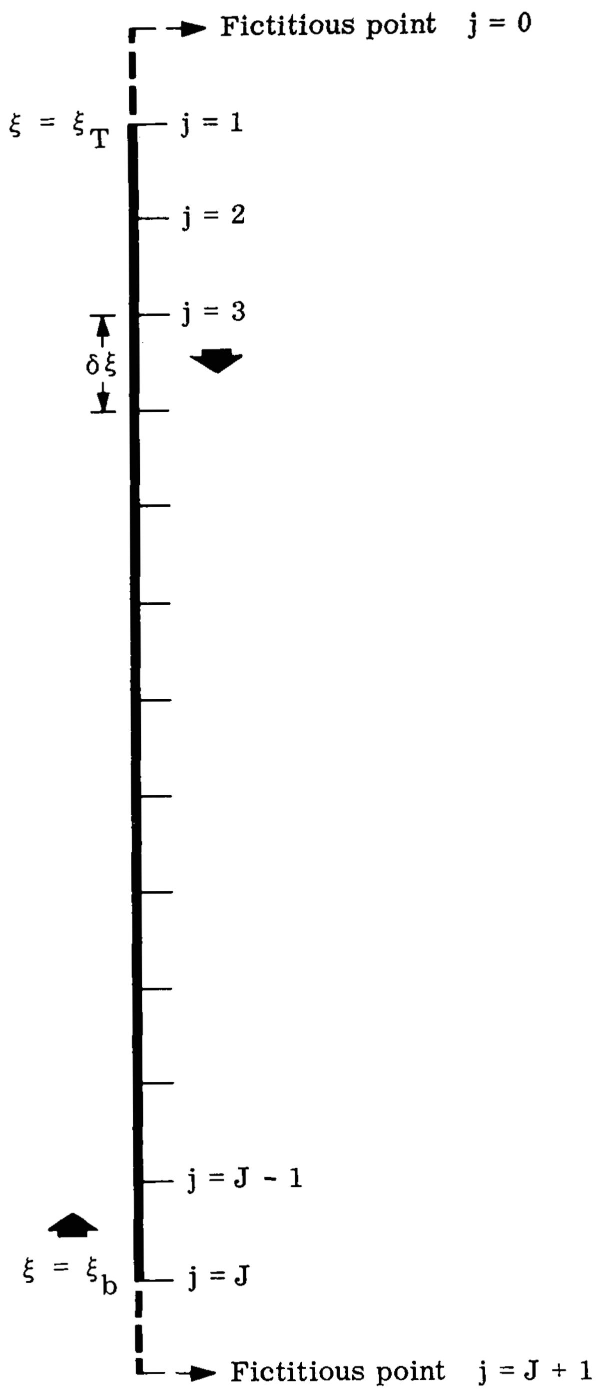

FIGURE 1.—Finite difference scheme.

From (5.1), (5.2), (6.1), (6.2) and (5a.1), (5a 2), (6a.1), (6a.2) we can inductively calculate E1N(j), E2N(j), F1N(j), and F2N(j) in order of increasing j (j=1, 2, 3 . . . J−1). Now we use the lower boundary condition to get $v_1(J)$ and $v_2(J)$.

C. APPLICATION OF THE LOWER BOUNDARY CONDITION

As in the case of upper boundary condition, we invoke Assumption 4, introduce a fictitious point at $J+1$, and write the boundary condition at J in the finite difference form. Thus we get

$$[\mathrm{A2N}(J)+\mathrm{C0N}(J)]v_1(J-1)+[\mathrm{B1N}(J)+\mathrm{A2N}(J)\cdot g\mathrm{L1N}]\cdot v_1(J)-[\mathrm{DFN}(J)+\mathrm{A2N}(J)\cdot h\mathrm{L1N}]+\mathrm{A2N}(J)\cdot\mathrm{FRN}(J)\cdot v_2(J)=0 \quad (5b)$$

$$[\mathrm{A2N}(J)+\mathrm{C0N}(J)]v_2(J-1)+[\mathrm{B1N}(J)+\mathrm{A2N}(J)\cdot g\mathrm{L2N}]\cdot v_2(J)-[\mathrm{EFN}(J)+\mathrm{A2N}(J)\cdot h\mathrm{L2N}]-\mathrm{A2N}(J)\cdot\mathrm{FRN}(J)\cdot v_1(J)=0 \quad (6b)$$

where,

$$\left.\begin{aligned} g\mathrm{L1N}&=2\cdot\delta\xi\cdot\tau_{\mathrm{K}}\cdot\frac{l\nu^2}{2m\pi}=g\mathrm{L2N}\\ \mathrm{FRN}&=2\cdot\delta\xi\cdot\tau_{\mathrm{K}}\cdot\frac{l\nu^2}{2m\pi}\\ h\mathrm{L1N}&=2\cdot\delta\xi\cdot\left[E_{\mathrm{K}}\cdot\frac{2m\pi}{l}h_2+N_{\mathrm{K}}H_1\right]\\ h\mathrm{L2N}&=2\cdot\delta\xi\cdot\left[-E_{\mathrm{K}}\cdot\frac{2m\pi}{l}\cdot h_1+N_{\mathrm{K}}H_2\right]\end{aligned}\right\}\text{at } j=J$$

We can write for $v_1(J-1)$ and $v_2(J-1)$ in (5b) and (6b),

$$v_1(J-1)=\mathrm{E1N}(J-1)\cdot v_1(J)+\mathrm{F1N}(J-1) \quad (5b.1)$$

$$v_2(J-1)=\mathrm{E2N}(J-1)\cdot v_2(J)+\mathrm{F2N}(J-1) \quad (6b.1)$$

Now substituting (5b.1) and (6b.1) in (5b) and (6b) we get

$$\mathrm{S1N}\cdot v_1(J)+\mathrm{S2N}+\mathrm{S3N}\cdot v_2(J)=0 \quad (5b.2)$$

$$\mathrm{S4N}\cdot v_2(J)+\mathrm{S5N}+\mathrm{S6N}\cdot v_1(J)=0 \quad (6b.2)$$

where

$$\mathrm{S1N}=[\mathrm{A2N}(J)\cdot\mathrm{E1N}(J-1)+\mathrm{C0N}(J)\cdot\mathrm{E1N}(J-1)+\mathrm{B1N}(J)+\mathrm{A2N}(J)\cdot g\mathrm{L1N}]$$

$$\mathrm{S2N}=[\mathrm{A2N}(J)\cdot\mathrm{F1N}(J-1)+\mathrm{C0N}(J)\cdot\mathrm{F1N}(J-1)-\mathrm{DFN}(J)-\mathrm{A2N}(J)\cdot h\mathrm{L1N}]$$

$$\mathrm{S3N}=+[\mathrm{A2N}(J)\cdot\mathrm{FRN}]$$

$$\mathrm{S4N}=[\mathrm{A2N}(J)\cdot\mathrm{E2N}(J-1)+\mathrm{C0N}(J)\cdot\mathrm{E2N}(J-1)+\mathrm{B1N}(J)+\mathrm{A2N}(J)\cdot g\mathrm{L2N}]$$

$$\mathrm{S5N}=[\mathrm{A2N}(J)\cdot\mathrm{F2N}(J-1)+\mathrm{C0N}(J)\cdot\mathrm{F2N}(J-1)-\mathrm{EFN}(J)-\mathrm{A2N}(J)\cdot h\mathrm{L2N}]$$

$$\mathrm{S6N}=-[\mathrm{A2N}(J)\cdot\mathrm{FRN}]$$

D. FINAL PHASE OF THE FINITE DIFFERENCE SOLUTION

From (5b.2) and (6b.2) we can very easily obtain v_1

(J) and v_2 (J) by direct elimination. After obtaining $v_1(J)$ and $v_2(J)$ we use (5) and (6) to calculate $v_1(j)$ and $v_2(j)$ inductively in the decreasing order of $j(j=J-1, J-2, \ldots 4, 3, 2, 1)$. Thus we arrive at the complete solution.

7. SOME COMPARATIVE RESULTS

For comparison purposes, we take Saltzman's [20] model, for which some results were published. Finite difference solutions for wave number $(m,n)=(3,0)$ are obtained. Figure 2 shows the solution for heating with friction while figure 3 gives the solution for mountain with friction. It should be noted that the origin of figure 2 corresponds to 45° longitude in Saltzman's figure. This is so because the heating maximum in figure 2 is at the origin, while it is placed at 45° longitude in Saltzman's figure (see corrigenda [20]). Here the grid spacing is arbitrarily taken as 5 mb. Experimentation with different grid spacings is contemplated. The time taken by the IBM–7090 is less than a minute for one solution for v_*, with all the related fields such as T_*, ω_*, and k_*. The agreement, at least for this type of atmospheric problem can be considered very satisfactory. The results with the second model of Saltzman [21] were equally successful but are not published here.

8. SOME EXPERIMENTAL RESULTS

Only the results of a few experiments will be discussed here. No attempt will be made, at present, to construct a general theory.

A. TOP BOUNDARY CONDITION

From figure 2, we can see that with $\omega_{*T}=0$ as the top boundary condition, we get very large perturbations at the upper boundary for certain harmonics. If the top boundary condition is changed to $v_{*T}=0$, which can be easily done in this numerical scheme, figure 4 is the result. Everything else is held the same as in figure 2. It is found that though this change in the upper boundary condition had an insignificant effect on the lower tropospheric perturbations, the values obtained for levels above 50 mb. appear to be more reasonable. So for all the remaining experiments the top boundary condition is taken as $v_{*T}=0$.

B. INFLUENCE OF THE SEASONAL CHANGE IN THE ZONAL MEAN STATE ON THE TOPOGRAPHICALLY FORCED PERTURBATIONS

To study the effect of zonal mean state change on the perturbations, produced by the mountains, we take the following data:

$$L=8.333\times10^7 \text{ cm.}$$
$$l=36$$
$$k=9$$
$$g=980 \text{ cm. sec.}^{-2}$$
$$R=2.87\times10^6 \text{ cm.}^{-2} \text{ sec.}^{-2} \text{ deg.}^{-1}$$
$$c_p=1.00\times10^7 \text{ cm.}^2 \text{ sec.}^{-2} \text{ deg.}^{-1}$$
$$C=1.6\times10^4 \text{ cm.}$$
$$p_s=1000 \text{ mb.}$$
$$p_b=900 \text{ mb.}$$
$$p_T=5 \text{ mb.}$$
$$h_*=h_1 \cos\frac{2\pi mX}{l}\cos\frac{2\pi nY}{k}$$
$$h_1=2\times10^4 \text{ cm.}$$
$$H_*=0$$
$$\rho_b=1.2\times10^{-3}\text{gm. cm.}^{-3}$$

Also the values of K_0, $\partial T_0/\partial Y$, and U_0 utilized here are given in table 1. At 30°N. and 60°N. the U_0 values at the lower boundary are arbitrarily taken as 1 m. sec.$^{-1}$ both in winter and summer (because it is not still clear how far we can trust the observational 900-mb. values at these latitudes). At 45°N., the U_0 values at the lower boundary are taken as 2.5 m. sec.$^{-1}$ and 4.5 m. sec.$^{-1}$, for summer and winter respectively, which appear to agree with the observations. f and β values are taken to correspond to the latitude under consideration. In all these figures corresponding to mountain with friction cases, the atmospheric troughs and ridges show a slight shift from the topographic troughs and ridges.

Figures 5 to 10 give the solutions for $(m, n)=(3,0)$ at different latitudes. The changes in the intensity of circulation and the position of the nodes are of interest in this type of study. It is to be noted that at 30°N. and 60°N. the node appears at a lower pressure in winter than in summer. At 60°N., this results in a reversal of phase even at 500 mb. from one season to the other. The analytical studies generally have restrictions on K_0 though they may be different for troposphere and stratosphere. To study the effect of this, a hypothetical K_0 (table 1, col. 1), which has constant values in the troposphere and stratosphere with a linear variation between 300 and 100 mb., is taken. This K_0 is used at all the latitudes for both the seasons keeping everything else the same. Figures 11–16 show the results which are self-explanatory. From these, we can conclude that for a quantitative theory of the stationary zonally asymmetric perturbations, the hypothetical vertical structure of the zonal mean stability is a good approximation in many cases. However, for 30°N. in the summer and for 60°N. in the winter, there are significant discrepancies, especially in the upper atmosphere above the 200-mb. level. Also in all these cases, one can see that the perturbations attain their maximum amplitudes near the stratosphere.

In order to get a rough qualitative explanation of these results, let us consider the following analogies. Equations (3) and (4) in this problem of forcing due to the moutains are similar (if Ξ, Θ, and $(\Lambda-\nu^2)$ remain positive constants and if the time axis is replaced by the ξ axis) to the equations expressing the free vibrations of a weight of mass Ξ, attached to a spring having an elastic constant $(\Lambda-\nu^2)$, in a viscous medium with a damping constant Θ. (We could also suggest an electrical analogy of a discharging condenser with a capacity of

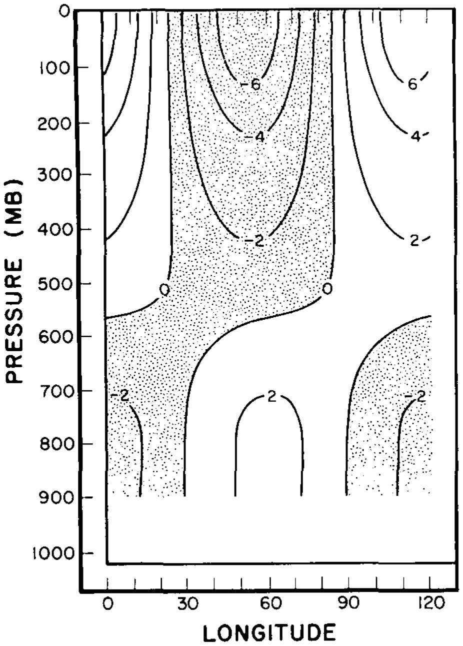

FIGURE 2.—v_* solution in m. sec.$^{-1}$ for Saltzman's [20] model. Heating with friction case. $(m,n)=(3,0)$. $\omega_*=0$ at the top.

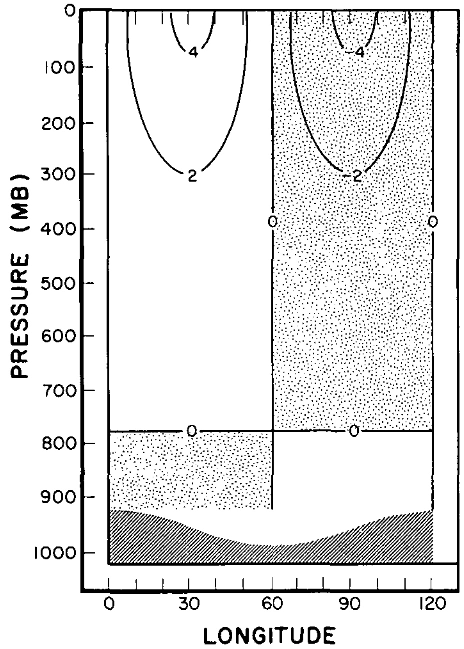

FIGURE 3.—v_* solution in m. sec.$^{-1}$ for Saltzman's [20] model. Mountain with friction case. $(m,n)=(3,0)$. $\omega_*=0$ at the top.

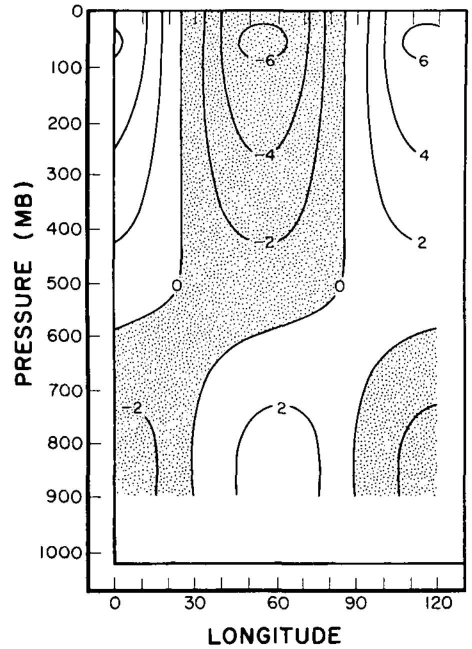

FIGURE 4.—v_* solution in m. sec.$^{-1}$ for Saltzman's [20] model. Heating with friction case. $(m,n)=(3,0)$. $v_*=0$ at the top.

$(\Lambda-\nu^2)^{-1}$, through an inductance Ξ and a resistance Θ.) In the atmosphere, for certain planetary scales of motion (e.g. $(m, n)=(3, 0)$), the coefficient $\Lambda-\nu^2$ is positive, though not a constant. Besides, the coefficients Ξ, and Θ are generally positive, though not constants, in the atmosphere. Thus for these scales of motion, falling back on the analogy suggested above, we can expect damped harmonic oscillations of v_l in ξ. This means for these scales it is possible to have nodes for v_* with respect to ξ, the number again depending on the coefficients and the boundary conditions. By virtue of the boundary condition at $\xi=\xi_T$ the origin is a node in this problem. In the spring analogy, the mass is at rest initially. So we can expect a maximum amplitude of v_* to occur at some distance from the origin. This "distance" (or in our analogy, the "interval") depends on the coefficients and the boundary condition at the other end. In this atmospheric problem, this point happens to be, in many cases, near the tropopause. As ξ increases, the perturbations are damped out, as suggested by our analogy. $(\Lambda-\nu^2)$

TABLE 1.—*Values of* K_0, $\partial T_0/\partial y$, *and* U_0 *utilized. Here,* K_0 *is in* 10^4 *CGS,* $\partial T_0/\partial y$ *is in* 10^{-3} *CGS,* U_0 *is in* 10^2 *CGS. W stands for winter, S for summer, HYP for hypothetical values,* p *for pressure in mb. Up to 100-mb. level,* K_0 *and* $\partial T_0/\partial y$ *values for summer and winter were computed from Peixoto's [17] standard-level data, assuming linear variation between the neighboring points for which the data are available for the use of centered differencing. Above 100-mb. level, these values are hypothetical.*

p	K_0HYP	30°N.						45°N.						60°N.					
		K_0W	K_0S	$\frac{\partial T_0}{\partial y}$W	$\frac{\partial T_0}{\partial y}$S	U_0W	U_0S	K_0W	K_0S	$\frac{\partial T_0}{\partial y}$W	$\frac{\partial T_0}{\partial y}$S	U_0W	U_0S	K_0W	K_0S	$\frac{\partial T_0}{\partial y}$W	$\frac{\partial T_0}{\partial y}$S	U_0W	U_0S
900	−2.00	−2.60	−2.13	−6.13	−3.53	1.00	1.00	−1.81	−2.03	−8.50	−5.90	4.68	2.50	−1.23	−1.81	−6.39	−5.20	1.00	1.00
800	−2.00	−2.15	−2.27	−5.50	−3.00	3.64	2.50	−1.93	−2.07	−7.57	−5.57	7.34	4.45	−1.64	−1.98	−4.87	−4.56	2.43	2.27
700	−2.00	−2.08	−2.30	−5.30	−2.60	6.48	3.97	−2.12	−2.15	−7.30	−5.10	10.18	6.49	−2.07	−2.15	−4.48	−4.44	3.85	3.63
600	−2.00	−2.10	−2.17	−5.40	−2.50	9.73	5.51	−2.21	−2.17	−6.90	−5.05	13.32	8.74	−2.08	−2.15	−4.24	−4.17	4.37	5.14
500	−2.00	−2.13	−2.10	−5.50	−2.40	13.64	7.27	−2.19	−2.15	−6.50	−5.00	16.83	11.37	−2.08	−2.16	−3.99	−3.90	7.08	6.81
400	−2.00	−1.57	−1.75	−5.10	−2.45	18.29	9.40	−1.65	−1.70	−5.80	−4.80	20.76	14.50	−1.40	−1.48	−3.54	−3.09	8.98	8.58
300	−2.00	−1.00	−1.31	−4.70	−2.50	23.82	12.20	−.95	−1.07	−5.10	−4.60	25.24	18.38	−.72	−.80	−3.09	−2.29	11.14	10.32
275	−1.63	−.90	−1.13	−4.15	−1.80	25.34	12.94	−.80	−.91	−3.28	−2.80	26.28	19.30	−.62	−.68	−2.05	−1.20	11.65	10.67
250	−1.16	−.80	−.95	−3.60	−1.10	26.79	13.48	−.65	−.75	−1.45	−1.00	26.93	19.82	−.52	−.56	−1.01	−.11	11.98	10.81
225	−.70	−.71	−.77	−3.05	−.40	28.17	13.79	−.53	−.60	.38	.80	27.08	19.84	−.41	−.44	.03	.98	12.10	10.70
200	−.33	−.62	−.60	−2.50	.30	29.45	13.81	−.40	−.45	2.20	2.60	26.64	19.26	−.31	−.32	1.08	2.06	11.94	10.29
175	−.33	−.51	−.47	−.28	1.55	30.17	13.32	−.33	−.39	3.40	3.60	25.57	18.07	−.27	−.28	1.03	2.68	11.63	9.57
150	−.33	−.40	−.35	1.95	2.80	29.64	11.99	−.26	−.33	4.60	4.60	23.79	16.25	−.23	−.24	.99	3.30	11.27	8.52
125	−.33	−.33	−.30	4.18	4.05	27.42	9.52	−.20	−.23	5.80	5.60	21.06	13.57	−.19	−.20	.94	3.91	10.87	7.02
100	−.33	−.25	−.25	6.40	5.30	22.74	5.39	−.15	−.12	7.00	6.60	16.95	9.66	−.16	−.16	.90	4.53	10.41	4.88
75	−.33	−.18	−.17	4.80	3.98	16.46	.18	−.11	−.09	5.25	4.95	11.93	4.92	−.12	−.12	.67	3.40	9.90	2.31
50	−.33	−.10	−.08	3.20	2.65	10.16	−5.04	−.07	−.05	3.50	3.30	6.90	.19	−.08	−.08	.45	2.26	9.39	−.27
25	−.33	−.05	−.04	1.60	1.33	3.86	−10.25	−.04	−.03	1.75	1.65	1.88	−4.54	−.04	−.04	.22	1.13	8.88	−2.84
5	−.33	−.01	−.01	.32	.27	−1.18	−14.43	−.01	−.05	.35	.33	−2.14	−8.33	−.01	−.01	.05	.23	8.47	−4.90

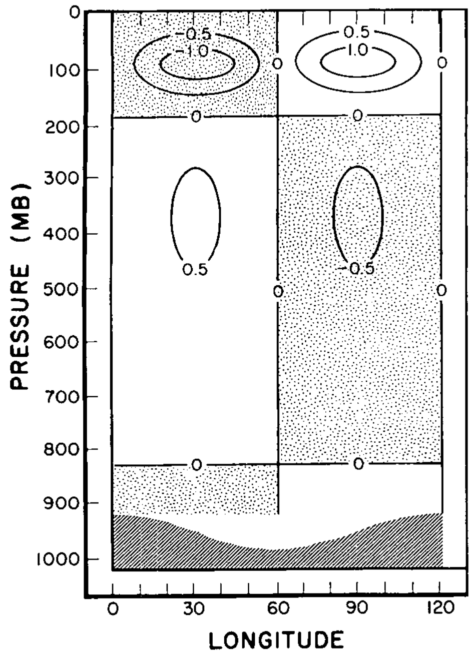

FIGURE 5.—$v*$ solution in m. sec.$^{-1}$ at 30° N. for summer. Zonal mean profiles taken from table 1. $(m,n)=(3,0)$. Mountain with friction case.

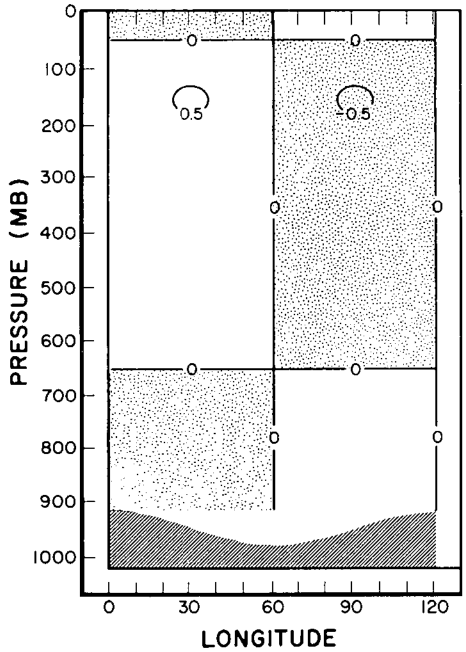

FIGURE 6.—$v*$ solution in m. sec.$^{-1}$ at 30°N. for winter. Zonal mean profiles taken from table 1. $(m,n)=(3,0)$. Mountain with friction case.

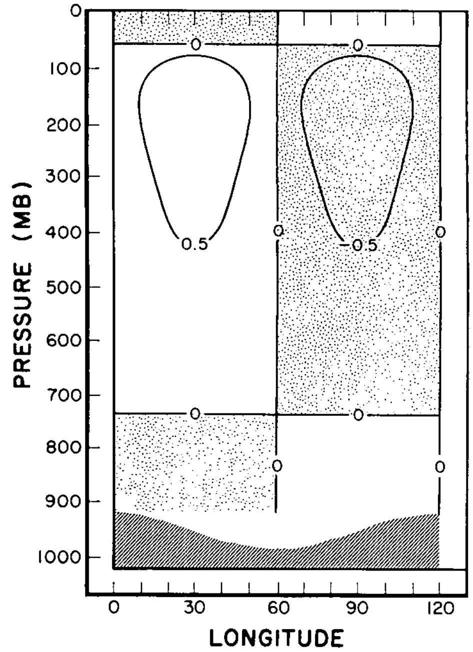

FIGURE 7.—$v*$ solution in m. sec.$^{-1}$ at 45°N. for summer. Zonal mean profiles taken from table 1. $(m,n)=(3,0)$. Mountain with friction case.

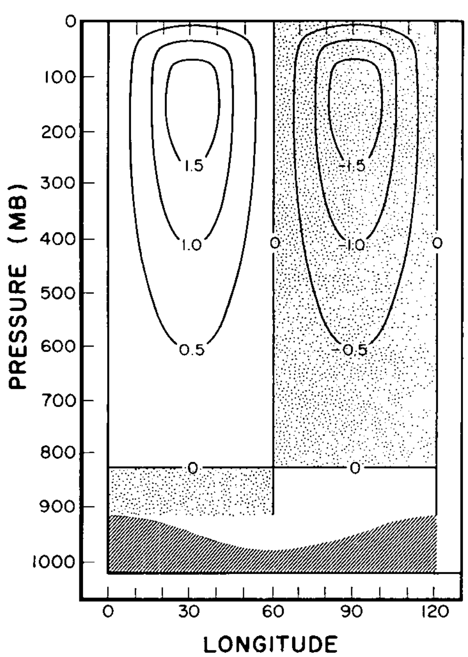

FIGURE 8.—$v*$ solution in m. sec.$^{-1}$ at 45°N. for winter. Zonal mean profiles taken from table 1. $(m,n)=(3,0)$. Mountain with friction case.

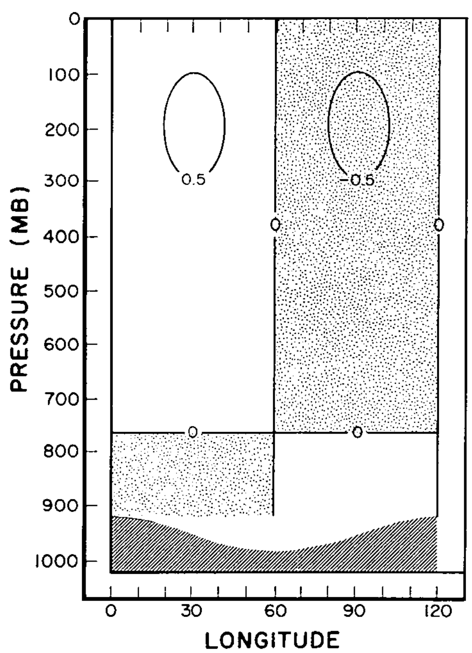

FIGURE 9.—$v*$ solution in m. sec.$^{-1}$ at 60°N. for summer. Zonal mean profiles taken from table 1. $(m,n)=(3,0)$. Mountain with friction case.

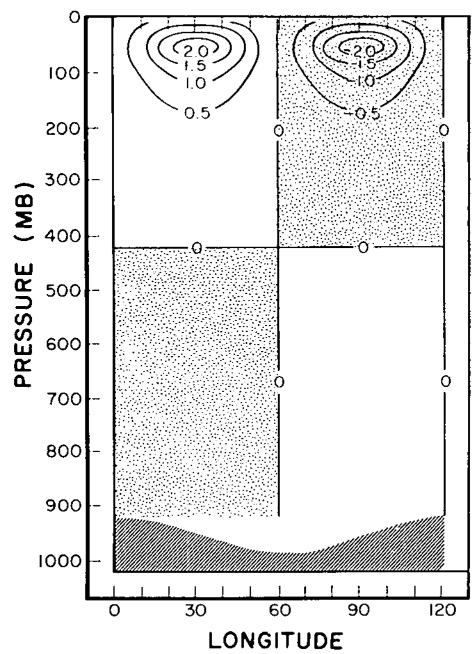

FIGURE 10.—$v*$ solution in m. sec.$^{-1}$ at 60°N. for winter. Zonal mean profiles taken from table 1. $(m,n)=(3,0)$. Mountain with friction case.

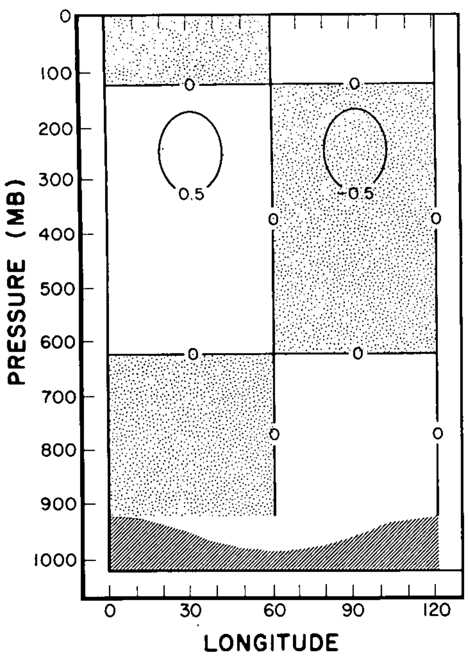

FIGURE 11.—$v*$ solution in m. sec.$^{-1}$ at 30°N. for summer. Hypothetical K_0 and other zonal mean profiles taken from table 1. $(m,n)=(3,0)$. Mountain with friction case.

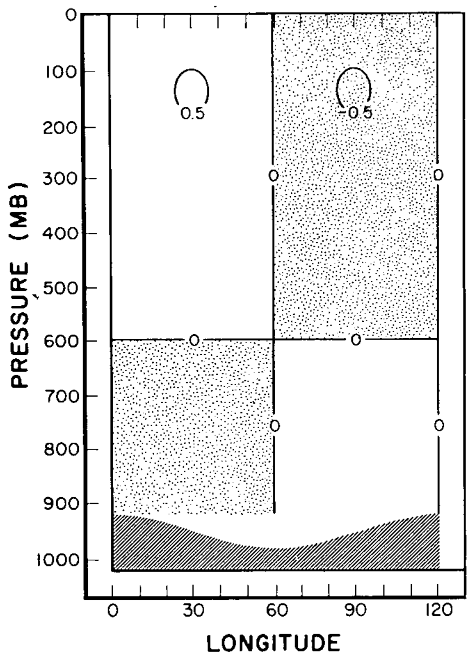

FIGURE 12.—$v*$ solution in m. sec.$^{-1}$ at 30°N. for winter. Hypothetical K_0 and other zonal mean profiles taken from table 1. $(m,n)=(3,0)$. Mountain with friction case.

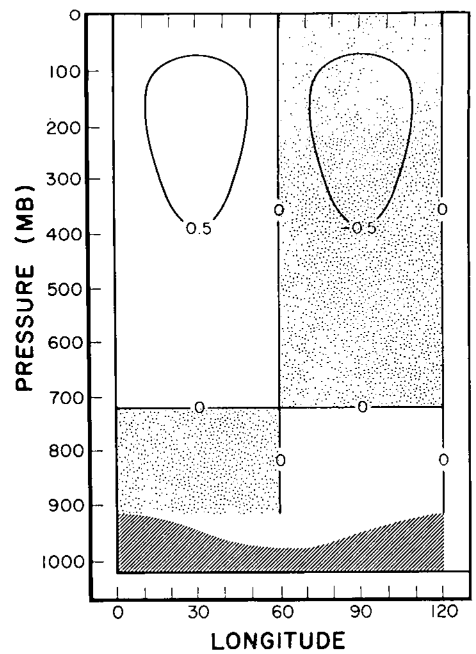

FIGURE 13.—$v*$ solution in m. sec.$^{-1}$ at 45°N. for summer. Hypothetical K_0 and other zonal mean profiles taken from table 1. $(m,n)=(3,0)$. Mountain with friction case.

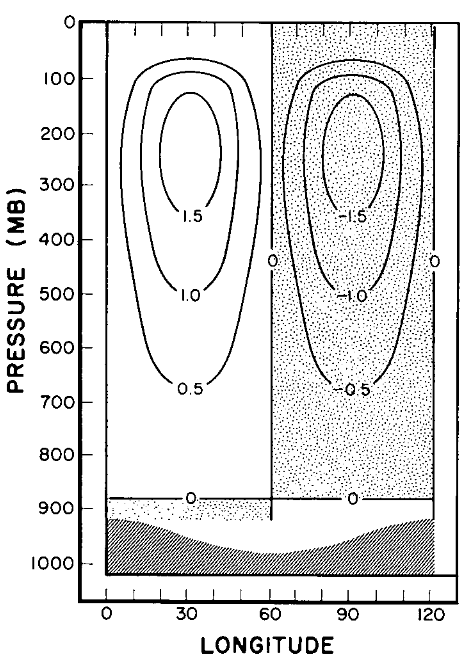

FIGURE 14.—$v*$ solution in m. sec.$^{-1}$ at 45°N. for winter. Hypothetical K_0 and other zonal mean profiles taken from table 1. $(m,n)=(3,0)$. Mountain with friction case.

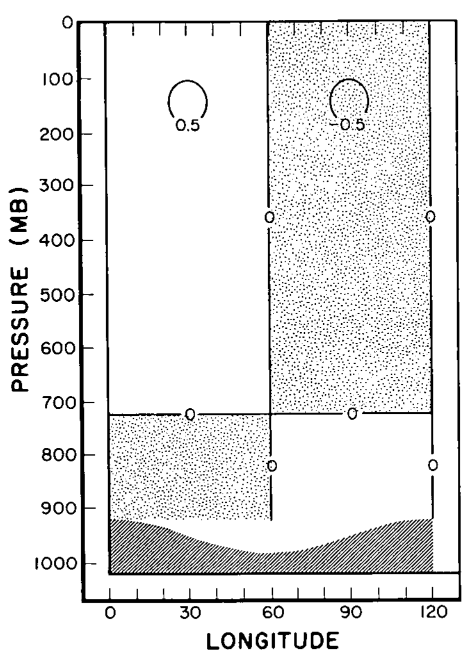

FIGURE 15.—$v*$ solution in m. sec.$^{-1}$ at 60° N. for summer. Hypothetical K_0 and other zonal mean profiles taken from table 1. $(m,n)=(3,0)$. Mountain with friction case.

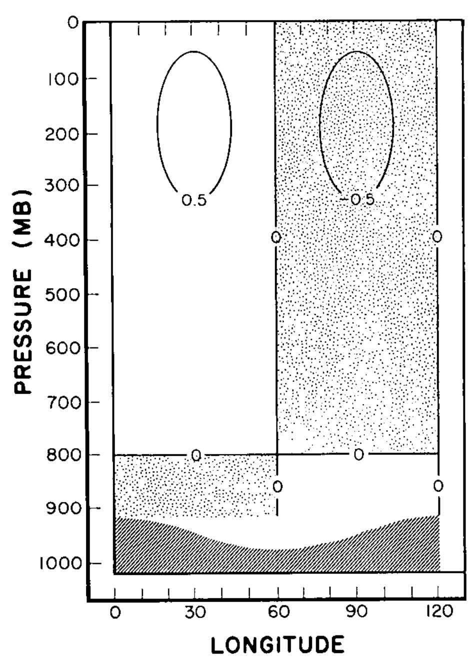

FIGURE 16.—$v*$ solution in m. sec.$^{-1}$ at 60° N. for winter. Hypothetical K_0 and other zonal mean profiles taken from table 1. $(m,n)=(3,0)$. Mountain with friction case.

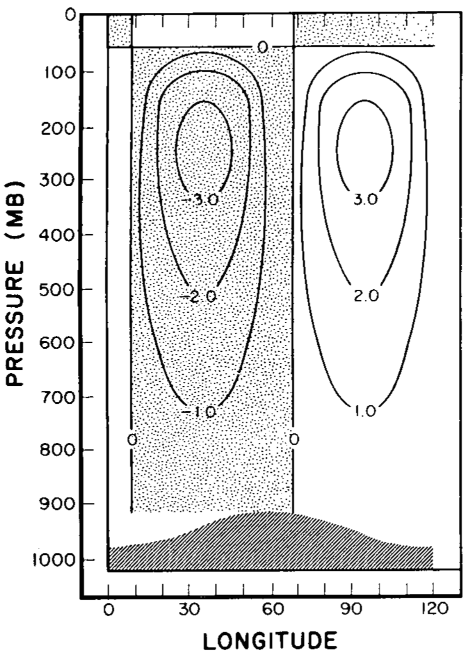

FIGURE 17.—$v*$ solution in m. sec.$^{-1}$ at 45° N. for summer. Zonal mean profiles taken from table 1. $(m,n)=(3,1)$. Mountain with friction case.

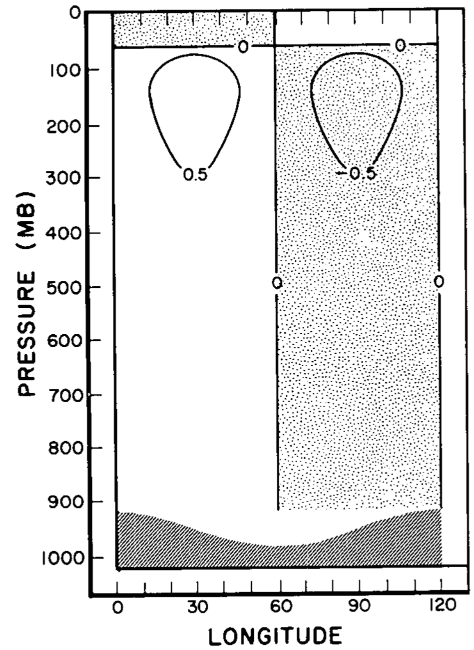

FIGURE 19.—$v*$ solution in m. sec.$^{-1}$ at 45° N. for summer. Uniform U_0 equal to that of the 500-mb. U_0 given in table 1 is used. K_0 values are taken from table 1. $(m,n)=(3,0)$. Mountain with friction case.

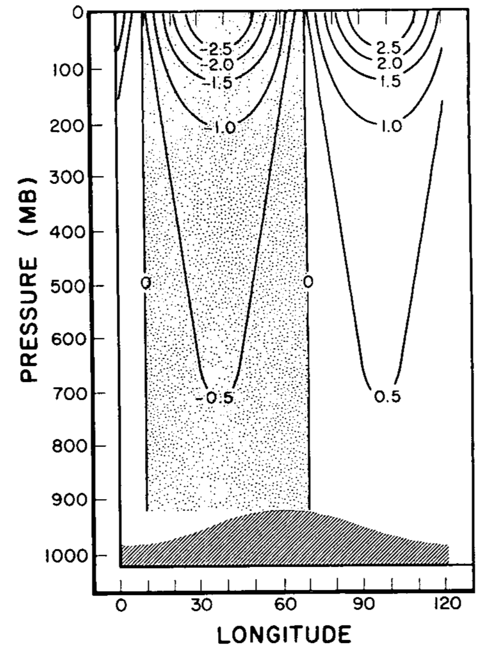

FIGURE 21.—$v*$ solution in m. sec.$^{-1}$ at 45° N. for summer. Uniform U_0 equal to that of the 500-mb. U_0 given in in table 1 is used. K_0 values are taken from table 1. $(m,n)=(3,1)$. Mountain with friction case.

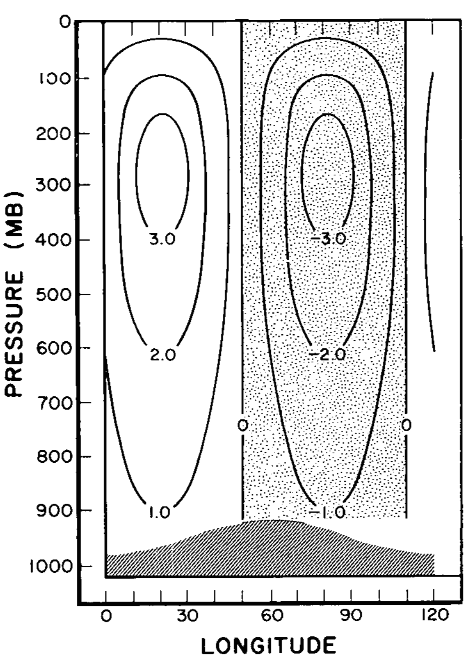

FIGURE 18.—$v*$ solution in m. sec.$^{-1}$ at 45° N. for winter. Zonal mean profiles taken from table 1. $(m,n)=(3,1)$. Mountain with friction case.

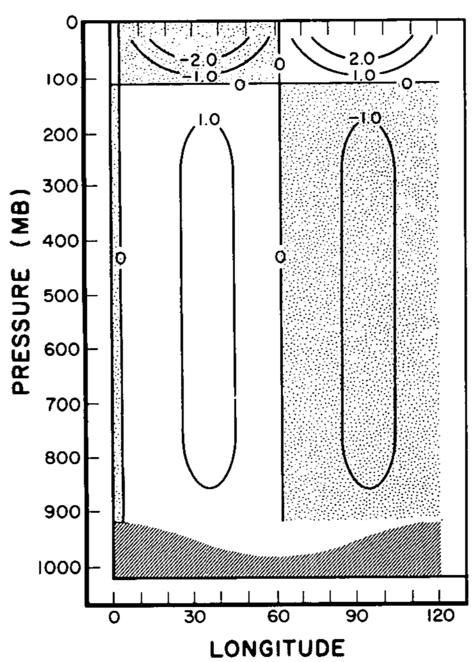

FIGURE 20.—$v*$ solution in m. sec.$^{-1}$ at 45° N. for winter. Uniform U_0 equal to that of the 500-mb. U_0 given in table 1 is used. K_0 values are taken from table 1. $(m,n)=(3,0)$. Mountain with friction case.

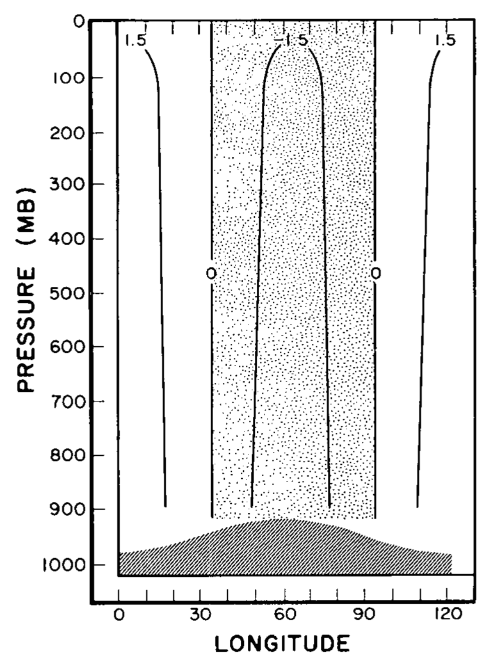

FIGURE 22.—$v*$ solution in m. sec.$^{-1}$ at 45° N. for winter. Uniform U_0 equal to that of the 500-mb. U_0 given in table 1 is used. K_0 values are taken from table 1. $(m,n)=(3,1)$. Mountain with friction case.

becomes negative, when the horizontal advection of relative vorticity dominates over the β advection term. In this case, depending on the other coefficients, the solution can become exponential and we cannot expect any nodes. For certain scales of motion, this happens to be the case. The point in the wave number space at which this switch occurs is close to the quasi-resonant point. The solutions exhibit a sudden change in character, while crossing this quasi-resonant point.

Now we shall go back to the discrepancies for 30° N. for summer and 60° N. for winter. For 60° N. in winter, the K_0 value at ξ_b is much smaller than the hypothetical K_0 value at ξ_b. This induces greater forcing at the boundary and this may be the reason for large discrepancies in the upper regions. For 30° N. in summer, no such obvious explanation can be given. In this context, the author feels that many more experiments can be designed to answer certain specific interesting questions.

Figures 17 and 18 show the results for $(m, n)=(3, 1)$ at 45° N. Significant phase changes from one season to the other at all levels are the interesting features of these figures. This can happen if the wave number falls on one side of the quasi-resonant frequency in one season and on the other side in another season (cf., Gilchrist [10]).

To investigate the acceptability of the barotropic or equivalent barotropic theories, a uniform current, with the 500-mb. zonal mean velocity at 45° N. corresponding to the season considered, is introduced. The forcing is kept the same by adjusting the mountain height. The results for $(m, n)=(3, 0)$ are given in figures 19 and 20. For $(m, n)=(3, 1)$, the results are given in figures 21 and 22. It can be inferred that the barotropic or equivalent barotropic theories can give only qualitative results even at the 500-mb. level for $(m, n)=(3, 1)$. At least for some important scales, they seem to be incapable of giving acceptable results. Also, from figures 21 and 22 we can infer, from the vertical structure of the response, that the wave number (3, 1) falls on either side of the quasi-resonant frequency according to the season, giving rise to a 40° phase change.

9. SOME CONCLUDING COMMENTS

The results here show the importance of the vertical structure of the zonal mean state and the scale of the perturbations and, therefore, have an important bearing on the numerical modeling of the atmosphere. Before trying to construct a quantitative theory in a spherical geometry, it will be of great interest to experiment with different kinds of heating functions. Above all, we should keep in mind that the nonseparability of (1), the complexity of the lower boundary condition, and our ignorance regarding the vertical structure of the perturbation heating function, are the formidable impediments in the way of constructing a quantitative linear theory.

ACKNOWLEDGMENTS

With pleasure, I thank Dr. Barry Saltzman for the keen interest he has shown in this work. My thanks are also due to Mr. Charles Gadsden for his aid in map analysis.

This research has been sponsored by the Weather Bureau, U.S. Department of Commerce, under contract Cwb–10763.

REFERENCES

1. E. W. Barrett, "Some Applications of Harmonic Analysis to the Study of the General Circulation, III," *Beiträge Zur Physik der Atmosphäre*, vol. 34, No. 314, 1961, pp. 167–197.
2. H. Bateman, *Higher Transcendental Functions*, vol. I, McGraw-Hill Book Co., Inc., New York 1953, pp. 1–302.
3. B. Bolin, "On the Influence of the Earth's Orography on the General Character of the Westerlies," *Tellus*, vol. 2, No. 3, Aug. 1950, pp. 184–195.
4. J. G. Charney and A. Eliassen, "A Numerical Method for Predicting the Perturbations of the Middle-Latitude Westerlies," *Tellus*, vol. 1, No. 2, May 1949, pp. 38–54.
5. P. F. Clapp, "Normal Heat Sources and Sinks in the Lower Troposhere in Winter," *Monthly Weather Review*, vol. 89, No. 5, May 1961, pp. 147–162.
6. J. F. DeLisle and J. F. Harper, "A Calculation of the Effect of Large-Scale Heat Sources on the Southern Hemisphere Subtropical Wind Flow," *Tellus*, vol. 13, No. 1, Feb. 1961, pp. 56–65.
7. B. R. Döös, "The Influence of Exchange of Sensible Heat with the Earth's Surface on the Planetary Flow," *Tellus*, vol. 14, No. 2, May 1962, pp. 133–147.
8. K. Gambo, "The Scale of Atmospheric Motions and the Effect of Topography on Numerical Weather Prediction in the Lower Atmosphere," *Papers in Meteorology and Geophysics*, vol. 8, No. 1, Apr. 1957, pp. 1–24.
9. K. Gambo, "The Topographical Effect upon the Jet Stream in the Westerlies," *Journal of the Meteorological Society of Japan*, Series 2, vol. 34, No. 1, Mar. 1956, pp. 24–28.
10. B. Gilchrist, "The Seasonal Phase Changes of Thermally Produced Perturbations in the Westerlies," *Proceedings of the Toronto Meteorological Conference, Sept. 9–15, 1953*, American Meteorological Society and Royal Meteorological Society, 1954, pp. 129–131.
11. B. Haurwitz and R. A. Craig, "Atmospheric Flow Patterns and Their Representation by Spherical-Surface Harmonics," *Geophysical Research Papers*, No. 14, Cambridge Research Center, U.S. Air Force, July 1952, 78 pp.
12. Y. Kawata, "The Influence of the Rocky Mountains on Non-Steady Isobaric Height Patterns," *Journal of the Meteorological Society of Japan*, Series 2, vol. 35, No. 3, June 1957, pp. 174–183.
13. H. L. Kuo, "Dynamic Instability of Two-Dimensional Nondivergent Flow in a Barotropic Atmosphere," *Journal of Meteorology*, vol. 6, No. 2, Apr. 1949, pp. 105–122.
14. H. L. Kuo, "Finite Amplitude Three-Dimensional Harmonic-Waves on the Spherical Earth," *Journal of Meteorology*, vol. 16, No. 5, Oct. 1959, pp. 101–111.
15. M. Magata, "On the Topographical Effect Upon the Perturbations of the Middle Latitude Westerlies," *Papers in Meteorology and Geophysics*, vol. 8, No. 1, Apr. 1957, pp. 25–38.
16. Y. Mintz, "Design of Some Numerical General Circulation Experiments," *Bulletin of the Research Council of Israel*, Section G, vol. 7, No. 2/3, Oct. 1958, pp. 67–114.
17. J. P. Peixoto, "Hemispheric Temperature Conditions During the Year 1950," *Scientific Report* No. 4, Contract No. AF 19(604)–6108, Dept. of Meteorology, Massachusetts Institute of Technology, 1960, 211 pp.

18. P. Queney, "The Problem of Air Flow over Mountains: A Summary of Theoretical Studies," *Bulletin of the American Meteorological Society*, vol. 29, No. 1, Jan. 1948, pp. 16–26.

19. R. D. Richtmyer, *Difference Methods for Initial-Value Problems*, Interscience Publishers, Inc., New York, 1957.

20. B. Saltzman, "A Generalized Solution for the Large-Scale Time Average Perturbations in the Atmosphere," *Journal of the Atmospheric Sciences*, vol. 20, No. 3, May 1963, pp. 226–235 (corrigenda, ibid,. vol. 20, No. 5, Sept. 1963, p. 465).

21. B. Saltzman, "On the Theory of the Winter-Average Perturbations in the Troposphere and Stratosphere," *Monthly Weather Review*, vol. 93, No. 4, Apr. 1965, pp. 195–211.

22. B. Saltzman and A. Fleisher, "Spectral Statistics of the Wind at 500 mb.," *Journal of the Atmospheric Sciences*, vol. 19, No. 2, Mar. 1962, pp. 196–204.

23. B. Saltzman and P. Peixoto, "Harmonic Analysis of the Mean Northern Hemisphere Wind Field for the Year 1950," *Quarterly Journal of the Royal Meteorological Society*, vol. 83, No. 357, July 1957, pp. 360–364.

24. B. Saltzman and M. Sankar-Rao, "A Diagnostic Study of the Mean State of the Atmosphere," *Journal of the Atmospheric Sciences*, vol. 20, No. 5, Sept. 1963, pp. 438–447.

25. M. Sankar-Rao, "Convergence Conditions for Relaxation Solution of a Class of Elliptic Equations," *Final Report*, General Circulation Research on Contract No. Cwb–10502, The Travelers Research Center, Hartford, 1963, pp. 1–8.

26. J. Smagorinsky, "The Dynamical Influence of Large-Scale Heat Sources and Sinks on the Quasi-Stationary Mean Motions of the Atmosphere," *Quarterly Journal of the Royal Meteorological Society*, vol. 79, No. 341, July 1953, pp. 342–366.

27. Staff Members, Academia Sinica, Institute of Geophysics and Meteorology, "On the General Circulation over Eastern Asia, III," *Tellus*, vol. 10, No. 3, Aug. 1958, pp. 299–312.

28. R. C. Sutcliffe, "Mean Upper Contour Patterns of the Northern Hemisphere—The Thermal-Synoptic View-Point," *Quarterly Journal of the Royal Meteorological Society*, vol. 77, No. 333, July 1951, pp. 435–440.

29. J. Van Mieghem, P. Defrise, J. Van Isacker, "Harmonic Analysis of the Normal Monthly Northern Hemisphere Geostrophic Flow at 500 mb.," Klasse der Wetenschappen, Vlaamische Academie voor Wetenschappen, *Mededelingen*, vol. 22, No. 4, 1960, 38 pp.

[*Received August 19, 1964; revised December 11, 1964*]